

# Mesoscopic and microscopic dipole clusters: Structure and phase transitions

A.I. Belousov and Yu.E. Lozovik\*

Laboratory of Nanophysics, Institute of Spectroscopy, Russian Academy of Sciences,  
Troitsk, 142092, Moscow region, Russia

Two dimensional (2D) classical system of dipole particles confined by a quadratic potential is studied. This system can be used as a model for rare electrons in semiconductor structures near a metal electrode, indirect excitons in coupled quantum dots etc. For clusters of  $N \leq 80$  particles ground state configurations and appropriate eigenfrequencies and eigenvectors for the normal modes are found. Monte Carlo and molecular dynamic methods are used to study in detail the order - disorder transition (the "melting" of clusters). In mesoscopic clusters ( $N < 37$ ) there is a hierarchy of transitions: at lower temperatures an intershell orientational disordering of pairs of shells takes place; at higher temperatures the intershell diffusion sets in and the shell structure disappears. In "macroscopic" clusters ( $N > 37$ ) an orientational "melting" of only the outer shell is possible. The most stable clusters (having both maximal lowest nonzero eigenfrequencies and maximal temperatures of total melting) are that of completed crystal shells which are concentric groups of nodes of 2D hexagonal lattice with a number of nodes placed in the center of them. The picture of disordering in clusters is compared with that in infinite 2D dipole system. The study of the radial diffusion constant, the structure factor, the local minima distribution and other quantities shows that the melting temperature is a nonmonotonic function of the number of particles in the system. The dynamical equilibrium between "solidlike" and "orientationally disordered" forms of clusters is considered.

PACS numbers: 61.46.+w, 68.65.+g, 36.40.Ei

## I. INTRODUCTION

Properties of a set of physical systems can, under certain conditions, be studied with the help of the model system of interacting dipoles. Particularly, it is a dipole - dipole interaction that is of main importance when small dielectric particles on a surface of electrolyte<sup>1</sup> or monolayers of adsorbed atoms<sup>2</sup> are considered. Another class of the systems in which the most part of interesting properties is due to a dipole character of interaction is the class of electron systems in semiconductors of small size located in the vicinity of a metal electrode electrostatic image forces can play an essential role. This role can become crucial, for example, for semiconductors with a small width of the forbidden band, for which image forces can induce a semiconductor - metal transition.<sup>3</sup> Indirect excitons with spatially separated electrons and holes in coupled quantum wells also interact by a dipole law, leading to the crystallization at intermediate concentrations.<sup>4,5</sup>

Properties of *infinite* two dimensional dipole systems have been intensively studied both theoretically<sup>6</sup> and with the help of computer simulations<sup>7</sup> (see also Ref. [8]). But the study of mesoscopic systems of interacting dipoles (dipole clusters) is also of a particular interest. Recent advances in the microlithography and one - electronics revived markedly an interest to systems of small number of particles, interesting with the strong structural sensitivity to the number of particles and unusual rearrangements with increasing temperature. Particularly in recent experiments of Ashoori et al.<sup>9</sup> the charging of a quantum dot was studied by the single electron capacitance spectroscopy method. One of the most intriguing results of these experiments was the observation of an unusual dependence of the chemical potential on

the particle number  $N$ , when the total energy of the dot as a function of  $N$  had a quasi - periodic component of a universal shape (i.e. the electron addition are group into bunches). This dependence was shown to be caused by geometric effects associated with a packing of the triangular lattice into the circular confinement.<sup>10</sup> It is obvious that if the dot of a large enough size is situated near a single metal gate the electrostatic image forces will play an important role and the long-range electron - electron Coulomb interaction potential will transform to the short-ranged dipole - dipole one between "composite" particles "electron + image charge". A plane microtrap of cooled atoms with (normal to the plane) dipole momenta induced by static electric field or by an electromagnetic standing wave could be another physical example of a dipole cluster. The value of the dipole momenta of trapped atoms can be controlled by varying the magnitude of the field or by tuning the field frequency. Yet another interesting example of a dipole cluster is a system of indirect excitons in vertically coupled semiconductor quantum dots (see e.g. Refs. [11,12]). Under certain conditions the system of indirect excitons can be considered as a classical dipole cluster in the parabolic confinement (see below). Such double dots systems are within the scope of current fabrication technology.

The consideration of different properties of dipole, Coulomb and logarithmic clusters provides also a possibility to study the role of the interaction potential in the shell structure of ground state configurations (at  $T = 0$ ) and in the hierarchy of melting temperatures. One of the most interesting tasks is the search for "magic", most stable clusters. By now the structure of magic number clusters has been most extensively studied by the example of Lennard - Jones ( $LJ$ ) systems that correspond, e.g., to noble gases atomic clusters.<sup>13-15</sup> Of some inter-

est is the question: does the set of distinctive properties of "magic" clusters correlate with the particular form of an interaction potential? It is important to realize the manner in which changing the type of interaction potential from two - parameter in  $LJ$  system to repelling one - parameter in a dipole system may reflect on the properties of appropriate "magic" clusters, on the character of disordering effects and on the possibility of coexistence phenomena.

In this paper we study in detail the ground state structure of 2D dipole clusters consisting of a finite number of particles and the picture of their melting with increasing temperature. It turns out that on the basis of the character of disordering ("melting") phenomena dipole clusters can be divided into "mesoscopic" and "macroscopic" groups. In "mesoscopic" clusters of small number of particles ( $N < 37$ ) there are *two* stages of disordering: *orientational intershell disordering* of different pairs of shells and, at greater temperatures, *radial* disordering when particles begin to interchange between shells. The spectral analysis of ground state configurations of small clusters shows that the value of the minimal frequency of normal vibrations correlates with characteristic temperatures of orientational disordering. Increasing of the temperature of large particle number clusters ( $N > 37$ ) leads to radial disordering and to disruption of the shell structure at a temperature which is a function of the distance from the center of the system. An analysis of a behavior of different thermodynamic properties, when the nonuniformity of the density is taken into account, enables us to make a conclusion about the strong dependence of the total melting temperature on a cluster position in a periodic Mendeleev - type table (i.e. on the distribution of particles over crystal shells of different symmetry). As an intermediate between mesoscopic and macroscopic systems the cluster of 37 particles is considered. The most interesting feature of this cluster is the presence of the temperature region of coexistence of "solidlike" and orientationally disordered forms. This behavior of the system with increasing temperature is much alike the picture of structural transitions in magic number atomic clusters.

The paper is organized as follows. In Sec. II we describe the model and briefly outline the methods that were used to find global minima configurations and to calculate different thermodynamic properties. Sec. III is devoted to the description and discussion of ground state configurations. We consider the "faceting" of clusters, the eigenvectors and eigenfrequencies for the normal modes. In Sec. IV we present the results from Monte Carlo (MC) and molecular dynamic (MD) simulations at different temperatures and system sizes. We consider two cases: "mesoscopic" ( $N < 37$ , see Sec. IV A) and "macroscopic" ( $N > 37$ , see Sec. IV B) clusters. Separately, as an intermediate case, in Sec. IV C we study the cluster of  $N = 37$  particles. Our conclusions are presented in Sec. V.

## II. THE MODEL. NUMERICAL SIMULATION

The exposition below concerns a cluster of indirect excitons in double semiconductor dots, but the analysis can be obviously extended to any other above - mentioned dipole system. Let us consider two vertically coupled 2D semiconductor dots of a characteristic linear size  $L$  that are spaced at  $h$  apart. Under laser pulse on the forbidden band frequency, a formation of indirect excitons that are bounded states of electrons and holes belonging to different dots is possible (see. works [ 11,12] and references therein). In this work we are interested in the case that the exciton radius  $a(h)$  is much smaller of the mean distance  $L/\sqrt{N}$  between them;  $a(h) \sim a_0^*$  at the interdot separation  $h < a_0^*$  and  $a(h) \sim a_0^{*1/4} h^{3/4}$  at  $h \gg a_0^*$  where  $a_0^* = \hbar^2 \kappa / (4m^* e^2)$  is effective Bohr radius of 2D exciton in a media with dielectric constant  $\kappa$ ,  $N$  stands for the (mean) number of excitons in the system. In addition we suppose that quantum effects in the cluster can be neglected in view of the condition  $k_b T \gg \hbar^2 N / (m^* L^2)$ .

Provided that conditions discussed above are fulfilled, excitons in quantum dots can be considered as 2D classical system of particles with unidirected dipole momenta  $d \approx 2eh/\kappa$ . A confinement potential can be chosen in a parabolic form with strength  $\alpha$ . The Hamiltonian for such a system have the form

$$H = \sum_{i < j} \frac{d^2}{|\mathbf{r}_i - \mathbf{r}_j|^3} + \alpha \sum_{i=1}^N |\mathbf{r}_i|^2$$

The Hamiltonian can be written in a dimensionless form if we express the coordinates and energy in the following units:  $r_0 = d^{2/5}/\alpha^{1/5}$ ,  $E_0 = \alpha r_0^2$ . In such units the Hamiltonian becomes

$$H = \sum_{i < j} \frac{1}{|\mathbf{r}_i - \mathbf{r}_j|^3} + \sum_{i=1}^N |\mathbf{r}_i|^2 \quad (1)$$

From here on all the results will be given in the units introduced above. When considering thermodynamic properties of the system we will use the dimensionless temperature  $T = k_b T / \alpha r_0^2$ .

To find out ground state configurations of (1) we applied the following methods:

- 1) *Classical simulated annealing* method (CSA).<sup>16</sup>
- 2) *Combined Monte Carlo + gradient search* method.

All of the results presented below (see Table I) were independently obtained with the help of these algorithms in order to improve the reliability of results. Of course, none of existing algorithms of searching for the global minimum of multidimensional function can guarantee that a configuration obtained is the global minimum one. In order to overcome this difficulty we considered as many as 200 random initial configurations. This approach made it possible to study local minima as well as appropriate regions of catchment ("relative weights" of local minima).

In view of intrinsic statistical nature of the *CSA* method, the problem of localization of the system in local minima is solved in this approach much more easy than in different gradient methods. When using *CSA*, the system is modelled at some artificially introduced temperature  $T(t)$  which is gradually decreased with the time  $t$  of experiment. This make it possible to simulate the thermal noise and delocalize a system from metastable states. By starting from sufficiently high temperature of  $T(t = 0) = 10$ , at each  $t$  we performed  $\sim 200$  MC steps per particle, whereupon the temperature was decreased as  $T(t + 1) = 0.98T(t)$ . The trial move  $x \rightarrow x + \delta x$  at each MC step was generated in accordance with Gaussian probability distribution  $\Pi(\delta x) \sim \exp(-\delta x^2/T(t))$ . This move was accepted with the probability  $p = \min\{1, \exp(-\Delta E/T(t))\}$ . To gain in the accuracy of results several hundreds of conjugate gradient steps were performed at the last stage of the algorithm.

It turned out that *CSA* is not as fast the algorithm as the *combined MC + gradient search* method. A search for minima within the last approach consists of repeated (up to  $10^4$  combined moves) applying of the following methods:

1) Classical random search<sup>17</sup> when the trial move  $x \rightarrow x + \delta x$  is accepted if it reduces the energy. The maximal size of the trial move  $\max\{|\delta x|\}$  was chosen automatically to assure the acceptance probability of a new configuration of 0.1.

2) Gradient search method  $x \rightarrow x - \gamma \nabla H$ ,  $\gamma \approx 0.01$ .

3) Ravine method.<sup>18</sup> In this method the direction  $l = x_m - x_1$  of the most probable displacement of the system that moves in a long narrow ravine is predicted on the basis of a series  $\{x_1, x_2, \dots, x_m\}$  of previously performed gradient search steps. A number of trial moves in this direction  $x \rightarrow 0.5(x_1 + x_2) + l\delta$  completes the method. The maximal size of these moves  $\max\{|\delta|\}$  was adjusted in such a way as to achieve the acceptance probability of  $\sim 0.1$ . We found that the throughout of the combined method was maximal when moves of above - mentioned types were performed in the ratio of  $N_1 : N_2 : N_3 = 100 : 10 : 2$ .

When studying the thermodynamic properties of the system, we used the Metropolis algorithm.<sup>19</sup> For the system of small number of particles ( $N < 40$ ) and at sufficiently low temperatures ( $T < 0.02$ ), when shells are well defined, we found it very efficient to perform collective MC moves of different shells. With the multigrid approach<sup>20</sup> for shell  $s$  of  $N_s$  particles one can apply the following types of collective moves with wave vector  $k_s$ :

1) angular perturbations such that angles  $\varphi_{i_s}$  of particles belonging to shell  $s$  vary as

$$\varphi_{i_s} \rightarrow \varphi_{i_s} + \xi \delta_\varphi(k; s) \cos(2\pi k i_s / N_s) \quad (2)$$

with  $\xi$  being the random variable uniform in  $[-1, 1)$ .

2) radial perturbations of shell  $s$ :

$$r_{i_s} \rightarrow r_{i_s} + \xi \delta_r(k; s) \cos(2\pi k i_s / N_s) \quad (3)$$

It is obvious that the case  $k_s = 0$  corresponds to the symmetrical "breathing" of shell  $s$  when the radial perturbation 2) is considered and to the rotation of the shell as a whole when one performs the global move of the first type. We found that such rotation of different shells was very important when studying the phenomena of inter-shell orientational disordering which take place in mesoscopic systems at low temperatures (the temperatures of orientational "melting" can be many orders less than temperatures of full disordering and shells destruction). The use of the collective moves described above enabled us to increase an efficiency of calculations, that is inversely proportional to the time needed to obtain a thermodynamic average with a given accuracy, about a five times.

Parameters  $\delta_\varphi$  and  $\delta_r$  (in Equations (2),(3)), as well as the maximum size of the Metropolis trial move, were adjusted in such a way as to hold the acceptance probability  $p_a \approx 0.4$ . To do this we averaged the acceptance probability  $\langle p \rangle$  of trial moves of different types ( $\langle p_r \rangle$ ,  $\langle p_\varphi \rangle$ ) in  $\sim 50$  MC steps per particle followed by the scaling  $\delta_\varphi(k; s) \rightarrow \delta_\varphi(k; s)(1 - p_a) / \langle p_\varphi \rangle$  (and analogous for  $\delta_r$ ).

To study dynamical characteristics of the system we applied the molecular dynamic simulation (both isokinetic and microcanonical methods where used). The main portion of the results presented below were obtained with the help of the fourth - order Runge - Kutta scheme. Equations of motion were integrated in  $\sim 10^4$  MD steps of size  $\tau \leq 0.01\tau_0$ , where  $\tau_0 = \sqrt{\alpha/m^*}$  determines the time scale in the system.

### III. GROUND STATE CONFIGURATIONS

Previous studies of Coulomb<sup>17,21</sup> and logarithmic<sup>22,23,24</sup> clusters have shown that it is suitable to classify these finite systems in accordance with their shell structure. An analysis of shell structures for different number of particles  $N$  enables one to consider the system as belonging to some period of a Mendeleev - type table. This table can be viewed as a classical equivalent to the well - known Periodic Table of elements. By studying regularities in this table the Coulomb clusters with a constant density of particles in each shell have been explored. This systems have been called "magic" Coulomb clusters. As examples of such systems clusters of 18 (1, 6, 11), 30 (5, 10, 15) and of 57 (1, 6, 11, 17, 22) particles have been proposed. The existence of magic clusters particularly manifests itself as cusps at a plot of excess energy  $\epsilon(N) = E(N)/N$  as a function of the number of particles. It have also been shown that these systems are more stable against intershell rotation.

Interaction between particles in a dipole cluster is more short - ranged with respect to that in Coulomb or logarithmic systems. Therefore it is possible to trace the role of the range of interparticle potential in the struc-

ture of 2D clusters, in the character of the formation of the Periodic Table and the type of shells (see also Ref. [10]). A difference between structures of dipole (D) and Coulomb clusters can be seen even at  $N = 10$  (the system  $D_{10}$  has the structure  $D_{10}(3, 7)$  as distinct from  $(2, 8)$  for Coulomb system.<sup>25</sup>) The number of differences grows rapidly with increasing the number of particles. To explore tendencies in the process of cluster shells developing, let us consider the shell configurations of 2D dipole clusters that are presented in Table I. The table shows that the basis for most configurations is provided by different parts of 2D hexagonal lattice. It should be noted that this observation is not specific to clusters with short - ranged interaction only. As was argued by Koulovskii and Shklovskii [10], only a narrow ring adjacent to the perimeter of sufficiently large Coulomb clusters is concentric to it, the rest of the cluster is filled with an almost perfect crystal.

When describing and analyzing the properties of such configurations we found it suitable to introduce into consideration the "crystal shells"  $Cr_c$  that are concentric groups of nodes of ideal 2D crystal with  $c$  nodes placed in the center of these groups (see Fig. 1). Obviously, in view of the axial symmetry of the confinement potential, we can concentrate on a finite number of the most symmetrical crystal shells.

By the number of particles in the center of the system, the crystal shells can be divided into the following groups:  $Cr_1, Cr_2, Cr_3, Cr_4$ . Fig. 1 explains our definition. The number of particles  $N_s$  that belong to crystal shell  $s$  (crystal row) of type  $Cr_c$  is  $N_s = c + 6(s - 1)$ . With the help of the crystal shell concept an analysis of the results presented in Table I shows that a formation of a "Periodic Table of elements" is done in accordance with the following *tendencies*:

1. The maximum number of *crystal shells* is filled.
2. The number of particles on the last two shells tends to be equal.

To illustrate these tendencies we underline the shells which are filled up (see Fig. 2 and Table I where types of basic crystal shells are also shown).

An addition of particles to the cluster leads to the completing of crystal shells of some type, followed by the structure rearrangement (see Fig. 2(c)-2(d)) after which a crystal shells of different type begins to fill. From Table I one can see that in some cases it is more advantageous to departure from the order  $Cr_1 \rightarrow Cr_2 \rightarrow Cr_3 \rightarrow Cr_4$  in which different types of crystal shells appear. Examples of such deviations (see  $D_{56} - D_{61}$  and  $D_{71} - D_{73}$ ) show that it can be profitable to reduce the number of particles on first shells (in the center of the system) and equalize them on the last ones. This observation underlines the importance of the requirement that the last two shells of the cluster have equal number of particles.

It is to be noted that for some systems the choice of the basis crystal group is ambiguous. The most spectacular

examples of this ambiguity are clusters that we assign to  $Cr_2$  crystal group (such clusters are  $D_{38}, D_{59}, D_{61}, D_{62}$ , see Table I and Fig. 3). Of course, one can consider these systems as having a number of partially completed crystal shells of  $Cr_4$  type (the "body" of a cluster) while the other particles locate on the surface of this "body". This approach is illustrated in Fig. 3 where two possible types of breakup of cluster  $D_{62}$  into shells is shown. In choosing between these possibilities we have being guided by the requirement the outer shell of the cluster to be well - defined and *closed*. For the system with a more short - ranged interaction potential (e.g. with the exponential or screened Coulomb interaction potential) it can be more natural to consider the evolution of the cluster with  $N$  as consisting of switching between *three* types of the most symmetrical basic crystal shells, namely  $Cr_1, Cr_3, Cr_4$ .<sup>10</sup> Seemingly, the question of what approach is more adequate can be answered on the data of the thermodynamic and dynamic analysis.

Results presented in Table I and above consideration enable us to suppose that for 2D dipole clusters a "period" of the Periodic Table consists of clusters with partially completed crystal shells of some symmetry (of some basic group). A role of "magic" clusters will be played by that with the *maximal number of completely filled crystal shells* and, in the case of clusters of large number of particles ( $N > 40$ ), with *equal number of particles on the two last shells*. An analysis of Table I suggests that dipole clusters  $D_{12}, D_{14}, D_{19}, D_{36}, D_{40}, D_{51}, D_{54}, D_{55}, D_{62}, D_{65}...$  can be considered as "magic" ones. Plots of the first and the second "derivatives" of specific energy  $\epsilon(N)$  with respect to number of particles  $N$  (see Fig. 4) can serve as illustrations of this assumption. The particle numbers at which cusps take place correlate with the "magic" numbers.

Somewhat ambiguous is the arrangements of particles into shells in the cluster  $D_{37}$  (see Fig. 5). We can see that one of the particles is between the second and the third shell to form an interstitial (it is analogous to the Frenkel defect in crystals). Such classification of this particle is based on the Voronoi analysis that shows that the central particle has six neighbors. The corresponding configuration can be denoted by  $D_{37}(\underline{1}, \underline{6}, \bar{1}, 13, 16)$  where the tilde stands for the interstitial. There exist also other opportunities to describe the structure of this cluster, for example as  $D_{37}(\underline{1}, \underline{6}, \underline{12}, \underline{2}, 16)$ . Our choice (see also Table I and Fig. 5(a)) is also proved itself in the results of the analysis of the lowest local minima configuration that has well - defined shell structure:  $D_{37}^{(1)}(1, 7, 13, 16)$  This configuration is shown in Fig. 5(). It should be noted that the cluster involved has a rather complex picture of disordering phenomena with increasing temperature. In the study of its thermodynamic properties presented below we show that the system  $D_{37}$  has properties that are characteristic of both small ( $N < 37$ ) and large ( $N > 37$ ) clusters.

Another region of distinctions from the above tenden-

cies in particle distribution throughout shells is a group of clusters  $D_{70} - D_{75}$  that have a pentagonal shape. It is possible that the size  $\Delta N$  of the region of non - hexagonal arrangement of  $N$  - particle cluster facets will be diminished with reducing the range of an interaction energy.

To obtain further information about the character of shells distribution in clusters of different number of particles we applied the spectral analysis of the ground state configurations (the spectral analysis of Coulomb clusters was performed in the work [ 21]). The main attention was given to the minimal nonzero eigenfrequencies  $\omega_{min}$  for the normal modes. Fig. 6 shows  $\omega_{min}$  as a function of the number of particles in the cluster. It is worthwhile to note that magic number clusters have maximal values of  $\omega_{min}$ . The correlation between the value of  $\omega_{min}$  and the extent to which crystal shells are completed is also seen.

One of the most interesting features of clusters is the strong dependence of their thermodynamic and dynamic properties on the number of particles  $N$ . An investigation of this dependence (see below) shows that dipole clusters can be divided into two groups: **1)** "mesoscopic" ("small") clusters,  $N < 37$ ; **2)** "macroscopic" ("large") clusters,  $N > 37$ . The intershell orientational disordering phenomenon is distinctive of mesoscopic clusters and does not take place in dipole clusters of a large number of particles. But differences between large and small clusters can be already seen when considering ground state configurations (at  $T = 0$ ).

Before of all, increasing the number of particles leads to the changes in the structure of lowest excitations, i.e. in the picture of eigenvectors with smallest nonzero frequencies. Shown in Fig. 7 are some characteristic examples of corresponding motions. Analogous to Coulomb clusters we found that small clusters with *incommensurate* number of particles in neighbor shells have the smallest eigenfrequencies  $\omega_{min}$ . The motion with minimal eigenfrequency  $\omega_{min}$  is then corresponds to intershell rotation<sup>21</sup> (see Fig. 7(a),(b)). When the number of particles is increased one can see that the picture of a motion with the minimal eigenfrequency evolves in such a way as to fall into a number of individual regions of "rotations" to form "vortex/antivortex pairs" (Fig. 7(c),(d)).

An interesting effect that accompany going from small to large clusters is the "facetting". Shells of mesoscopic clusters have near - circular shape, while an addition of particles leads to the developing of well - defined facets. This tendency is clearly seen in Fig. 8 in which the dependence of the measure of facetting  $\nu_s$  on  $N$  for different cluster shells  $s$  is presented. If shell number  $s$  of the cluster consists of particles with numbers  $\{i_1, i_2, ..i_N\}$ , then the parameter  $\nu_s$  can be defined as

$$\nu_s = \frac{\max_{i_s}\{|\mathbf{r}_{i_s}|\}}{\min_{i_s}\{|\mathbf{r}_{i_s}|\}} \quad (4)$$

From Fig. 8 one can see that with increasing the number

of particles, the shape of the cluster shells approach that of the crystal shells defined above (appropriate values of the parameter  $\nu_s$  are also shown by thick solid lines). In support of the fact that shells of small clusters have near - circular form, Fig. 8 shows that minimal differences between values of parameter  $\nu_s$  for crystal and cluster shells take place when the most symmetrical crystal shell  $Cr_1$  is being filled (see  $D_{17} - D_{19}, D_{32} - D_{36}$ ). Instead, this difference is maximal for clusters belonging to the other periods of "Mendeleev table" (i.e. of  $Cr_2, Cr_3, Cr_4$  basic groups).

#### IV. PHASE TRANSITIONS

Studying thermodynamic and dynamic properties of 2D dipole clusters, we explored the temperature region  $T < 1$  and calculated the following quantities:

- 1) Radial distribution function  $g(r)$ .
- 2) Pair and radial deviations:

$$\delta_{pair} = \frac{2}{N(N-1)} \sum_{i < j} \left[ \frac{\langle |\mathbf{r}_i - \mathbf{r}_j|^2 \rangle}{\langle |\mathbf{r}_i - \mathbf{r}_j|^2 \rangle^2} - 1 \right]^{1/2} \quad (5)$$

$$\delta_r = \frac{1}{N} \sum_i \left[ \frac{\langle |\mathbf{r}_i|^2 \rangle}{\langle |\mathbf{r}_i|^2 \rangle^2} - 1 \right]^{1/2},$$

$$u_r^2 = \frac{1}{N} \sum_i \left[ \langle |\mathbf{r}_i|^2 \rangle - \langle |\mathbf{r}_i| \rangle^2 \right] \quad (6)$$

**3)** Radial diffusion constant  $\mathcal{D}_r$ . This quantity changes drastically in the region of temperatures that is appropriate to the radial disordering of the cluster and to the interchange of particles between different shells. For it is beyond reason to believe that a hydrodynamical approach is valid for such small systems, we found it incorrect to define the diffusion constant via a Fourier - image of the velocity autocorrelation function. Instead, this quantity was estimated from equation

$$\langle \Delta r^2 \rangle = 2\mathcal{D}_r t + c \quad (7)$$

where  $\langle \Delta r^2 \rangle = \frac{1}{N} \sum_{i=1}^N [|\mathbf{r}_i(t)| - |\mathbf{r}_i(0)|]^2$  is a radial mean square displacement of a particle in time  $t$  (in units of  $\tau_0$ , see above),  $c$  is some constant.

**4)** Local minima distribution  $\rho(\epsilon_{loc})$ . In order to estimate this histogram and to determine the relative occupancy of different minima on the potential energy surface, at each step of measurements several hundred steps of the gradient minimization (see above) was come out to determine the nearest local minimum.

In simulations of macroscopic clusters we found it helpful to calculate the following quantities:

**5)** The number  $d_n(R_c)$  of particles which are in a circle of radius  $R_c$  and have  $n$  nearest neighbors. The Voronoi

construction was applied to find nearest neighbors of each particle.

### 6) Static structure factor $S(\mathbf{k})$

$$S(\mathbf{k}) = \frac{1}{N} \langle \rho_{\mathbf{k}} \rho_{-\mathbf{k}} \rangle,$$

$$\rho_{\mathbf{k}} = \sum_{i=1}^N \exp(j\mathbf{k}\mathbf{r}_i), \quad j^2 = -1 \quad (8)$$

A usual way of studying the intershell orientational disordering in clusters is an analysis of relative angle deviations of shells, in analogy with quantities (5) - (6). In this approach the temperature  $T_{s_1 s_2}$  of orientational "melting" of shells  $s_1$  and  $s_2$  of a cluster is defined as that at which there is a sharp increase in the value of appropriate relative angle deviations. We follow a different method of finding the disordering temperature  $T_{s_1 s_2}$  as that at which the *mutual orientational (order) parameter* of shells  $s_1$  and  $s_2$  vanishes. We define this quantity as follows: for each shell  $s$  of  $N_s$  particles we consider complex - valued quantity  $\psi_s$ :

$$\psi_s = \frac{1}{N_s} \sum_{i_s} \exp(jN_s \varphi_i) \quad (9)$$

The sum in (9) is extended over all particles possessed by shell  $s$ . The *mutual orientational (order) parameter* is then defined as

$$g_{s_1 s_2} = \langle \psi_{s_1} \psi_{s_2}^* \rangle \quad (10)$$

It is obvious, that  $g_{s_1 s_2}$  disappears at the point of relative disordering (slipping) of shells  $s_1$  and  $s_2$  (in the vicinity of this the very point there will be also a sharp increase in relative angle deviations). The quantity  $g_{ss} = \langle |\psi_s|^2 \rangle$  will be a measure of the intrashell order. We note that quantities  $\psi_s$  and  $g_{s_1 s_2}$  are analogous to orientational parameter  $\psi_6$  and correlation function  $g_6(r)$  in infinite 2D system, where vanishing (when the translational order is absent) of the correlation function,  $g_6(r) \rightarrow 0$  as  $r \rightarrow \infty$ , indicates the relative orientational disordering of distant parts of a system.

### A. Mesoscopic clusters

The distinctive property of mesoscopic clusters is the presence of *two types* of disordering effects in these systems:<sup>17,24,25</sup> an intershell orientational disordering (an orientational melting of shells  $s_1$  and  $s_2$  at temperature  $T_{s_1 s_2}$ ) and a radial disordering (a total melting at temperature  $T_f$  that is larger than any one of orientational melting temperatures). An analysis of eigenfrequencies and eigenvectors for the normal modes of small clusters shows that the motions with small lowest nonzero eigenfrequencies  $\omega_{min}$  correspond to intershell rotation (see Fig. 7). Such clusters will have small temperatures  $T_{s_1 s_2}$  of intershell disordering, at which shells start to

rotate relative to each other losing their mutual orientational order. Note that, in contrast to the case of large clusters, an intershell melting in small clusters takes place for *all* pairs of shells, i.e. there exist "melting" temperatures  $T_{21}, T_{32}, T_{43} \dots$ . In clusters of large number of particles ( $N > 37$ ) an orientational disordering of only the outer shell is possible. An analogous observation was made for Coulomb clusters.<sup>21</sup>

Shown in Fig. 9(b) are dependencies of the values of mutual orientational parameters  $g_{21}$  and  $g_{32}$  vs. temperature for three - shell cluster  $D_{24}$ . Pair and radial deviations  $\delta_{pair}(T)$  and  $u_r^2(T)$  (see (5),(6)) are also plotted. This figure shows that for cluster  $D_{24}$  one can define two temperatures  $T_{32} = (5 \pm 0.5) \cdot 10^{-4}$  and  $T_{21} = (3 \pm 0.05) \cdot 10^{-4}$  that correspond to orientational melting of shells  $\{3, 2\}$  and  $\{2, 1\}$ .

Fig. 9(b) (see also Fig. 10) shows that pair and radial deviations (5), (6) are also sensitive to intershell rotation. One can see the regions of sharp increases in the values of these quantities that coincide with the regions of vanishing of mutual orientational order. The sensitivity of radial and pair deviations to the orientational disordering is due to the "breathing" of the cluster shells on their rotation. This breathing can be clearly seen if one trace the motion of a system along a "reaction path",<sup>26</sup> the most probable (of the weakest ascent in  $2N$  - dimensional space) trajectory which is appropriate to the intershell rotation.

Temperature  $T_{32} \approx 0.05 \pm 0.003$  of the orientational "melting" of the third shell of four - shell cluster  $D_{35}(1, 6, 12, 16)$  is only slightly lower than the temperature  $\overline{T_f} = 0.065 \pm 0.005$  of the total melting at which the radial order disappears (see Fig. 10). It is obvious that the temperature of an orientational intershell disordering will to a large extent depend on the distribution of particles throughout shells. Particularly, when the particle numbers in neighbor shells  $s_1$  and  $s_2$  are *commensurate*, temperature  $T_{s_1 s_2}$  of an orientational "melting" should be maximal (irrespective of whether these shells are inside the cluster or a pair of external shells is considered). Calculations do show that an addition of as little as one particle to small cluster  $D_{19}(1, 6, 12)$  with completely filled crystal shells of  $Cr_1$  type leads to abrupt decreasing of temperature  $T_{32}$  of orientational "melting". Indeed, temperature  $T_{32} \approx 0.03 \pm 0.002$  of  $D_{19}$  cluster is very nearly equal to that of the total melting  $T_f \approx 0.038 \pm 0.003$  (at which particles begin to interchange between shells). System  $D_{20}(1, 7, 12)$  becomes orientationally disordered at much smaller temperatures  $T_{32} < 5 \cdot 10^{-6}$ .

### B. Macroscopic clusters

The most interesting when considering macroscopic clusters (at  $N > 37$ ) is the question about the manner in which their melting temperatures  $T_f$  approach the tem-

perature  $T_c^{inf} = k_b T / (d^2 n^{3/2}) = 0.089 \pm 0.002$  of first order phase transition in 2D infinite dipole system (here  $n$  stands for the density of particles in the system).<sup>6,7</sup> But this analysis is made difficult by an uncertainty in the concept of the "density" of a cluster. This uncertainty does not enable us to use the natural for infinite systems unit of length  $a = 1/\sqrt{n}$ . When converting from "cluster" to "infinite system" temperature, one can introduce a *mean* density of a system as  $n = N/\pi R^2$  where  $R$  is the radius of the cluster. The uncertainty in  $R$  leads to the ambiguity of such definition of the cluster density. Moreover, if we deal with a cluster of a large enough number of particles the density will considerably vary with the distance to the center of the system. We will discuss this question in some more detail below.

To define an effective (mean) density of a cluster of not very large number of particles ( $N < 50$ ), when the nonuniformity of the density pointed out above is not essential, we made use of calculations of the static structure factor (8). Let us consider the distance  $|\delta\mathbf{k}|$  to the maximum of the structure factor, i.e. to the first Bragg peak for a "solid" cluster (when  $T < T_f$ ) or to the Lorentz peak in the case of a "liquid" cluster (when  $T > T_f$ ). The characteristic distance between particles in a cluster can be defined then as  $a = 2\pi/|\delta\mathbf{k}| = [2/(n\sqrt{3})]^{1/2}$ . In such a manner the corresponding temperature of 2D infinite system can be estimated as

$$T^{inf} = \frac{k_b T}{D^2 n^{3/2}} \approx T \frac{1}{0.8} \left[ \frac{|\delta\mathbf{k}|}{2\pi} \right]^3 \quad (11)$$

It turned out that for systems  $D_{36} - D_{52}$  the estimation  $T \approx T^{inf}$  works with a reasonable accuracy.

One of the most representative quantities for 2D infinite dipole system is excess energy  $\epsilon$  that exhibits a jump of  $\Delta\epsilon \approx 0.04$  at a temperature of phase transition  $T_c^{inf}$ .<sup>7</sup> Our calculations show (see Fig. 11) that such a sharp increase in an excess energy *does not take place* at least for clusters with  $N < 50$ .

Yet another quantity that is commonly used in analyzing phase transitions in infinite systems is structure factor  $S(\mathbf{k})$ , Eq. (8). The lattice to liquid transition is identified through the vanishing of the first Bragg peak  $S(\mathbf{k})$ ,  $\mathbf{k} \approx \mathbf{q}_1$ . We found that the magnitude of this peak (the maximum of the structure factor in the region  $|\mathbf{k}| > k_c \sim \pi$ ) is acutely sensitive to the disordering in clusters. The peak at small wave vectors  $|\mathbf{k}| < \pi$  that exists at any temperature due to finite size of the system involved is of no interest. Some characteristic examples of the behavior of the structure factor as a function of temperature are given in Fig. 12.

An independent quantity a sharp change in which testifies about the order/disorder transition is the radial diffusion constant  $\mathcal{D}_r$ , see equation (7). Fig. 13 presents the results of calculations of this quantity, performed for clusters  $D_{39}$ ,  $D_{40}$  and  $D_{45}$ . Each data point in this figure was obtained by averaging over results of 5 independent experiments in which the evolution of the system was

observed in a time that is typical for the diffusion of a particle for a distance of  $\Delta r \sim 1$ . The result of one of such experiments is shown in the insert of the figure.

An analysis of temperature dependencies of above quantities (5) - (8) enables us to plot the total melting temperature  $T_f(N)$  as a function of the number of particles in the cluster. This curve is shown in the insert of Fig. 14. Also shown are temperatures  $T_f^{inf}(N)$  of corresponding infinite system that are estimated with the help of Formula (11). Fig. 14 enables us to point out some characteristic features of the  $N$  dependence of the disordering temperature. **i)** Melting of all clusters studied takes place at temperatures much more smaller than temperature  $T_c^{inf} \approx 0.1$  of the phase transition in an infinite system. **ii)** The most interesting peculiarity of function  $T_f(N)$  is that it is nonmonotonic. Most likely, this peculiarity is primarily connected with the fact that a cluster of  $N$  particles can be considered as a part of a *strongly deformed* crystal lattice. Hence one studies the melting of a part of imperfect crystal with "frozen-in" interstitials and dislocations (see Fig. 2(a)), the melting temperature being a function of the number of such defects (of the value of an initial deformation of a cluster as a part of crystal). Obviously, the number of defects in the ground state configuration will be minimal in the case of "magic" cluster (see above) with a maximal number of filled crystal shells. An analysis of the data presented in Table I and in Fig. 14 shows that (at least for  $N < 52$ ) the "magic" clusters do have anomalously high melting temperatures.

Of course, the melting temperature is not a strictly defined quantity for finite systems. It makes sense to consider an interval  $\Delta T(N)$  of temperatures in which the disordering takes place. For clusters of large number of particles that repel each other and are in a confinement potential there is another, more important, reason that does not enable us to introduce a concrete melting temperature of a phase transition (of a total disordering). The point is that large clusters (at  $N > 50$ ) are irregular in both the density of particles and the density of defects. These densities can vary appreciably with the distance  $r$  to the center of the system<sup>27</sup> to lead to a strong  $r$  dependence of the melting temperature.

Let us consider this dependencies in some more detail. Results of numerical simulations show that large clusters can be divided into the following regions:<sup>10</sup> **(a)** the "core" of a cluster, a region adjacent to the center of the island and filled with a number of completed crystal shells; **(b)** the "layer of defects", the ring in which dislocations and disclinations are situated and which is "concentric" to the surface of the cluster; **(c)** the region between the surface of the island and the layer of defects. One can assume that temperatures of disordering in the regions considered above will differ greatly. Our calculations approve this assumption. As an example, we calculated the number of disclinations  $d_n(r)$  and the radial diffusion constant  $\mathcal{D}_r(r)$  as functions of the

distance  $r$  to the center of the cluster  $D_{80}$ . It turned out that temperature  $T_f^{inf}(r < r_c)$  of the disordering of a "core", the part of the cluster belonging to the circle of the radius  $r_c \approx 2.5$ , was independent of  $r$ :  $T_f^{inf}(r < 2.5) \approx 0.07 \pm 0.01$ . This temperature is slightly below  $T_c^{inf}$ . One may suppose that as  $N$  increases, the scaled temperature of core disordering  $T_f^{inf}(N; r < r_c)$  approaches the temperature of phase transition in 2D infinite dipole system:  $T_f^{inf}(N; r < r_c) \rightarrow T_c^{inf}$ ,  $N \rightarrow \infty$ .

The melting in other two regions of the cluster appeared to take place at much less temperature:  $T_f^{inf}(r > r_c) = 0.01 \pm 0.005$ . Obviously, the temperature of disordering in regions **(b)** and **(c)** will strongly depend on the number of disclinations and dislocations in the layer of defects (in the region **(b)**) as well as on the strength of initial deformations in the region **(c)**. Thus we argue that:

**i)** defined as a point of drastic changes in pair and radial deviations, diffusion constant and of disappearance of the first Bragg peak, neither "melting" temperature  $T_f(N)$  nor scaled to 2D infinite system melting temperature  $T_f^{inf}(N)$  tends to first - order phase transition temperature in infinite 2D system as the number of particles in the cluster increases.

**ii)** The function  $T_f^{inf}(N)$  (as well as  $T_f(N)$ ) is not monotonic. The magic number clusters, having minimal number of defects, have maximal melting temperatures.

**iii)** One can introduce the temperature  $T_f^{inf}(N; r < r_c) \rightarrow T_c^{inf}$ ,  $N \rightarrow \infty$  which is the (scaled to 2D infinite system) melting temperature of a core, the free of defects central region of a cluster.

These qualitative predictions are presented in Fig. 14.

### C. Cluster $D_{37}$

As have been pointed out above, system  $D_{37}$  can be considered as an intermediate one between mesoscopic and macroscopic clusters. An analysis of the global minimum configuration (see Fig. 5) and of the structure of normal motion with the minimal eigenfrequency  $\omega_{min}$  leads to the seemingly unambiguous conclusion about the absence of the intershell orientational disordering. However, our calculation shows that the melting in this system is not one - step process; instead, the orientational melting takes place at the temperature  $T = T^* \approx 0.01$  that is approximately three times lower than that of total melting  $T_f \approx 0.03 \pm 0.005$ . The orientational disordering of *all* pairs of shells takes place at temperature  $T^*$ .

The reason of this "anomalous" behavior of cluster  $D_{37}$  can be elucidated by considering the structure of the lowest local minima configurations (i.e. the configurations with the lowest energy). We have noted above (see Fig. 5(c)) that global and local minima configurations differ in a *symmetry*, namely, any breaking of the ground state configuration down into shells leads to the

necessity of viewing one or two particles (see Chapter III) as interstitials interposed between shells of the cluster. Only two first shells are well defined:  $D_{37}(1, 6, \dots)$ . On the contrary, the configuration of the first excited state (of the lowest local minima with energy  $\epsilon_{loc}^{(1)} \approx 8.3325$ ) is rather symmetrical and has the clear shell structure:  $D_{37}^{(1)}(1, 7, 13, 16)$ . As shells of the cluster in this local minimum are not faceted, it is not surprising that the motion (in this local minimum) with the lowest eigenfrequency  $\omega_{min}^{(1)} \approx 0.4$  corresponds to the intershell rotation. This is illustrated in Fig. 5(c).

Plotted in Fig. 15 is the probability of the central particle having six neighbors. This quantity can be defined as  $d_6(0.5)$ , see above. Fig. 15 shows that at temperatures  $T > T^* = 0.01 \pm 0.002$  there is a finite probability to find a system in the vicinity of the local minimum  $D_{37}^{(1)}(1, 7, \dots)$ . Yet another illustration of this rearrangement is the change in histogram  $\rho(\epsilon_{loc})$  of the local minima distribution shown in the insert of Fig. 15. One can see that at  $T = T^*$  a pike at energy  $\epsilon_{loc}^{(1)}$  appears. Further increasing the temperature leads to the occupancy of others local minima and, at  $T > 0.3$ , the radial disordering takes place, particles interchange between shells and the radial distribution function is washed out (see Fig. 15,16). So, at  $T > T^*$ , a part of time the system lives in the neighborhood of the "symmetrical" local minimum that is *unstable* against intershell rotation at such high temperatures. This intershell disordering also manifests itself as a sharp increase in relative angular intershell deviations at this the very temperature  $T = 0.01$ .

From results of studies of atomic clusters<sup>13,14</sup> it is known that clusters of some specific number of particles (so called "magic" *LJ* clusters such as  $LJ_{13}$ ,  $LJ_{19}$ , see work [15] and references therein) have distinct regions of coexistence of "liquidlike" and "solidlike" forms. In a certain temperature interval there is nonzero probability to find the cluster either in a "liquidlike" or in a "solidlike" form. It was shown that this unusual property owes its origin to features of the multidimensional potential energy surface and stems from an existence of regions (well - separated by high barriers) in phase space with distinct physical properties and appreciable residence time for the system in each region.

A picture of disordering in cluster  $D_{37}$  with increasing temperature closely resembles the picture of structural transitions in magic number atomic clusters. Of course, at sufficiently high temperatures, at  $T > T^* = 0.01$ , the system can be found in one of two distinct regions in phase space with a barrier between them. This equilibrium can be described as:

$$D_{37}(\underline{1}, 6, \tilde{1}, 13, 16) \xrightleftharpoons{K} D_{37}(1, 7, 13, 16),$$

$$K = \frac{[D_{37}(1, 7, 13, 16)]}{[D_{37}(\underline{1}, 6, \tilde{1}, 13, 16)]} = e^{-\Delta F(T)/T}$$

where  $\Delta F(T)$  is free energy difference of "symmetrical"



and "fully ordered" states of the cluster. At  $T < 0.01$  constant of equilibrium  $K \sim 1 - d_6(0.5)$  is equal to zero and increases markedly as the temperature is increased (see Fig. 15).

The analysis above shows that, with the cluster  $D_{37}$  being radial ordered, the region  $0.01 < T < 0.03$  *can not* be considered as the region of coexistence of its "solidlike" and "liquidlike" forms. Instead, this temperature interval can be thought of as the region of coexistence of "solidlike" and "orientationally disordered" forms. It is the presence of such region that enables us to consider the system  $D_{37}$  as an intermediate one that has features of both mesoscopic and macroscopic clusters.

To conclude of this paragraph we note that the number of  $D_{37}$  - like "anomalous" systems can be varied by tuning the characteristic range of an interaction potential. Increasing the temperature in such systems can lead to structure rearrangements (with changes in symmetry), changes in the shell distribution or in types of defects. Consequently, above consideration can be helpful in the study of thermodynamic properties of the clusters, parameters of interparticle potential of which can be varied in wide limits, e.g. of dusty plasma clusters,<sup>28,29</sup> of the system of electrons in a semiconductor dot with near metal electrodes,<sup>9,10</sup> etc.

## V. CONCLUSION

We have presented the results of a numerical simulation of finite 2D dipole system in the parabolic confinement. Ground state configurations and the spectrum of normal modes of clusters of  $N \leq 80$  particles have been found. An addition of particles to the system leads to a gradual filling of crystal shells of different symmetry. The clusters with minimal energies and maximal lowest eigenfrequencies ("magic" clusters) are that with the maximal number of completely filled crystal shells and (in the case of large clusters,  $N > 40$ ) with equal numbers of particles on the last two shells. Such clusters have also well developed facets.

The character of disordering with increasing the temperature is markedly different for mesoscopic ( $N < 37$ ) and macroscopic ( $N > 37$ ) clusters. Particularly, mesoscopic clusters are characterized by an existence of two types of disordering effects: orientational and full (radial). Depending on the degree to which crystal shells are completed the temperatures of orientational "melting" of different pairs of shells can differ greatly from each other. Orientational melting in large systems is absent.

An analysis of the local minima distribution of the system  $D_{37}$  as a function of temperature have shown that this system has features of both mesoscopic and macroscopic clusters. Namely, there is a region of temperatures in which cluster is in a dynamical equilibrium between "solidlike" and radial ordered but orientationally disordered forms.

The system of large number of particles is nonuniform: both the characteristic interparticle distance and the density of defects are functions of a distance  $r$  from the center of the system. As a consequence, the temperature at which a sharp increase in radial and pair deviations, vanishing of the first Bragg peak take place and the diffusion of particles appear does not approach temperature  $T_c^{inf}$  of first - order phase transition in 2D infinite dipole system as the number of particles is increased. Scaled to infinite system, "melting" temperature  $T_f^{inf}(N)$  is a nonmonotonous function of the number of particles and is maximal for magic number clusters. By taking into account the  $r$  dependence of the interparticle distance, the melting of the "core" of the cluster (i.e. its free of defects central region  $r < r_c(N)$ ) can be mapped to the melting of 2D infinite system with appropriate scaled temperature  $T^{inf}(N; r < r_c) \rightarrow T_c^{inf}$  as  $N$  increases.

## Acknowledgments

We wish to thank A.M. Popov and S.A. Verzakov for fruitful discussion. The work has been supported by Russian Foundation of Basic Research, INTAS and the Program "Physics of Solid Nanostructures".

---

\* e-mail: lozovik@isan.troitsk.ru

- <sup>1</sup> P. Pilranski, Phys. Rev. Lett. **45**, 8 (1980).
- <sup>2</sup> L.A. Bol'shov et. al., Uspekhi Fiz. Nauk (in Russian) **122**, 125 (1977).
- <sup>3</sup> V.M. Agranovich and Yu.E. Lozovik, JETP Lett. **17**, 148 (1972); I.V. Lerner and Yu.E. Lozovik, Phys. Lett. A **64**, 483 (1978); Yu.E. Lozovik and V.N. Nishanov, Fiz. Tv. Tela (Sov. Solid St. Phys.) **18**, 1905 (1976).
- <sup>4</sup> Yu.E. Lozovik and O.L. Berman, JETP Lett. **64**, 573 (1996).
- <sup>5</sup> X.M. Chen and J.J. Quinn, Phys. Rev. Lett. **67**, 895 (1991).
- <sup>6</sup> Yu.E. Lozovik and V.M. Farztdinov, Sol. St. Comm. **54**, 725 (1985); Yu.E. Lozovik, V.M. Farztdinov, B. Abdullaev and S.A. Kucherov, Phys. Lett. A **112**, 61 (1985).
- <sup>7</sup> V.M. Bedanov, G.V. Gadiyak and Yu.E. Lozovik, Phys. Lett. A **92**, 400 (1982).
- <sup>8</sup> A.T. Skjeltorp, Phys. Rev. Lett. **51**, 2306 (1983).
- <sup>9</sup> R.C. Ashoori et. al., Phys. Rev. Lett. **68**, 3088 (1992); **71**, 613 (1993); N.B. Zhitenev et. al., preprint cond-mat/9703241 (1997).
- <sup>10</sup> A.A. Koulakov and B.I. Shklovskii, Phys. Rev. B **57**, 2352 (1998).
- <sup>11</sup> A. Zrenner et. al., Phys. Rev. Lett. **72**, 3383 (1994); L.V. Butov, A. Zrenner, G. Abstreiter, G. Bohm and G. Weimann, Phys. Rev. Lett. **73**, 304 (1994); L.V. Butov et. al., Phys. Rev. B **52**, 12153 (1995).
- <sup>12</sup> Yu.E. Lozovik and N.E. Kaputkina, Phys. Scr. **57**, 542

- (1998).
- <sup>13</sup> D.J. Wales and R.S. Berry, Phys. Rev. Lett. **73**, 2875 (1994); **63**, 1156 (1989); R.M. Lynden-Bell and D.J. Wales, J. Chem. Phys. **101**, 1460 (1994).
- <sup>14</sup> C. Chakravarty, J. Chem. Phys. **103**, 10663 (1995).
- <sup>15</sup> T.L. Beck, J. Jellinek and R.S. Berry, J. Chem. Phys. **87**, 545 (1987).
- <sup>16</sup> S. Kirkpatrick, C.D. Gelatt Jr and M.P. Vecchi, Science **220**, 671 (1983).
- <sup>17</sup> Yu.E. Lozovik, Uspekhi Fiz. Nauk (in Russian), **153**, 356 (1987); Yu.E. Lozovik and V.A. Mandelshtam, Phys. Lett. A **145**, 269 (1990); **165**, 469 (1992).
- <sup>18</sup> N.N. Kalitkin, *Numerical Methods* (in Russian), (Nauka, Moskow, 1978).
- <sup>19</sup> *Monte Carlo Methods in Statistical Physics*, ed by K. Binder (Springer-Verlag, Berlin 1978).
- <sup>20</sup> A. Goodman and D. Sokal, Phys. Rev. D **56**, 1024 (1987).
- <sup>21</sup> V.M. Bedanov and F.M. Peeters, Phys. Rev. B **49**, 2662 (1994); V. Schweigert and F.M. Peeters, Phys. Rev. B. **51**, 7700 (1995); I.V. Schweigert, V.A. Schweigert and F.M. Peeters, Phys. Rev. B **54**, 10827 (1996).
- <sup>22</sup> R. Calinon et al. in *Ordering in Two Dimensions*, ed. S.K. Sinha (Elsevier, New York, 1980).
- <sup>23</sup> Y. Kondo et. al. Phys. Rev. Lett. **68**, 3331 (1992); G.E. Volovik and U. Parts, JETP Lett. **58**, 774 (1993).
- <sup>24</sup> Yu.E. Lozovik and E.A. Rakoch, Phys. Rev. B **57**, 1214 (1998).
- <sup>25</sup> Yu.E. Lozovik and E.A. Rakoch, Phys. Lett. A **235**, 55 (1997).
- <sup>26</sup> W. Quapp, Chem. Phys. Lett. **253**, 286 (1996).
- <sup>27</sup> The procedure considered above of the estimation of the effective density of small clusters (11) can be easily extended to the case of large systems. To define mean density  $n(r)$  of the cluster as a function of  $r$  one can consider structure factor  $S(\mathbf{q}; r, \delta r)$  of a part of the system that belongs to ring  $r \pm \delta r$  containing at least three shells of the cluster.
- <sup>28</sup> C.H. Chiang and L. I, Phys. Rev. Lett. **77**, 646 (1996).
- <sup>29</sup> A.P. Nefedov, O.F. Petrov, V.E. Fortov, Uspekhi Fiz. Nauk (in Russian), **167**, 1215 (1997).

Table I.

Ground state configurations of 2D dipole clusters  $D_N$  in a harmonic confining. Shown are shell configurations  $\{N_1, N_2, \dots\}$ , types of crystal shells (see in Text) and excess energy  $\epsilon = E/N$ .

$N$	$\{N_1, N_2, \dots\}$	$\epsilon$	$N$	$\{N_1, N_2, \dots\}$	$\epsilon$
1	1	0	41	<u>3,9,14,15</u>	$Cr_3$ 8.93397
2	2	0.64660	42	<u>3,9,14,16</u>	$Cr_3$ 9.08148
3	3	1.01394	43	<u>3,9,15,16</u>	$Cr_3$ 9.22705
4	4	1.38021	44	<u>3,9,15,17</u>	$Cr_3$ 9.37309
5	5	1.75713	45	<u>4,10,15,16</u>	$Cr_4$ 9.51691
6	1,5	2.04829	46	<u>4,10,15,17</u>	$Cr_4$ 9.66006
7	<u>1,6</u>	$Cr_1$ 2.32591	47	<u>4,10,16,17</u>	$Cr_4$ 9.80303
8	1,7	$Cr_1$ 2.63542	48	<u>4,10,16,18</u>	$Cr_4$ 9.94353
9	2,7	$Cr_2$ 2.92373	49	1,5,11,16,16	$Cr_1$ 10.08318
10	3,7	$Cr_3$ 3.19012	50	<u>1,6,11,16,16</u>	$Cr_1$ 10.21803
11	3,8	$Cr_3$ 3.41972	51	<u>1,6,12,16,16</u>	$Cr_1$ 10.35593
12	<u>3,9</u>	$Cr_3$ 3.66665	52	<u>1,6,11,17,17</u>	$Cr_1$ 10.49035
13	4,9	$Cr_4$ 3.89493	53	<u>1,6,12,17,17</u>	$Cr_1$ 10.62096
14	<u>4,10</u>	$Cr_4$ 4.13543	54	<u>1,6,12,17,18</u>	$Cr_1$ 10.75525
15	5,10	4.35999	55	<u>1,6,12,18,18</u>	$Cr_1$ 10.88617
16	1,5,10	4.56558	56	<u>1,6,12,18,19</u>	$Cr_1$ 11.02094
17	<u>1,6,10</u>	$Cr_1$ 4.77272	57	<u>1,6,12,18,20</u>	$Cr_1$ 11.15521
18	<u>1,6,11</u>	$Cr_1$ 4.97257	58	<u>1,6,12,18,21</u>	$Cr_1$ 11.28939
19	<u>1,6,12</u>	$Cr_1$ 5.18009	59	<u>2,8,13,18,18</u>	$Cr_2$ 11.41878
20	1,7,12	$Cr_1$ 5.38833	60	3,8,13,18,18	$Cr_3$ 11.54741
21	2,7,12	$Cr_2$ 5.59048	61	<u>2,8,14,18,19</u>	$Cr_2$ 11.67875
22	<u>2,8,12</u>	$Cr_2$ 5.77969	62	<u>2,8,14,19,19</u>	$Cr_2$ 11.80329
23	3,8,12	$Cr_3$ 5.96866	63	3,8,14,19,19	$Cr_3$ 11.92863
24	3,8,13	$Cr_3$ 6.14713	64	<u>3,9,14,19,19</u>	$Cr_3$ 12.05160
25	<u>3,9,13</u>	$Cr_3$ 6.32561	65	<u>3,9,15,19,19</u>	$Cr_3$ 12.17598
26	4,9,13	$Cr_4$ 6.50834	66	<u>3,9,14,20,20</u>	$Cr_3$ 12.30108
27	4,9,14	$Cr_4$ 6.68410	67	<u>3,9,15,20,20</u>	$Cr_3$ 12.42251
28	<u>4,10,14</u>	$Cr_4$ 6.85654	68	<u>3,9,15,20,21</u>	$Cr_3$ 12.54674
29	5,10,14	7.03598	69	<u>4,10,15,20,20</u>	$Cr_4$ 12.66865
30	5,10,15	7.20543	70	5,10,15,20,20	12.78866
31	1,5,10,15	$Cr_1$ 7.36745	71	1,5,10,15,20,21	12.90960
32	<u>1,6,12,13</u>	$Cr_1$ 7.52917	72	<u>4,10,16,21,21</u>	$Cr_4$ 13.03147
33	<u>1,6,12,14</u>	$Cr_1$ 7.68741	73	1,5,11,16,20,20	13.15305
34	<u>1,6,12,15</u>	$Cr_1$ 7.84408	74	1,5,11,16,21,20	13.27021
35	<u>1,6,12,16</u>	$Cr_1$ 8.00361	75	1,5,11,16,21,21	13.38454
36	<u>1,6,12,17</u>	$Cr_1$ 8.16885	76	<u>1,6,11,16,21,21</u>	$Cr_1$ 13.50135
37	<u>1,6,1,13,16</u>	$Cr_1$ 8.33111	77	<u>1,6,12,18,20,20</u>	$Cr_1$ 13.61939
38	<u>2,8,13,15</u>	$Cr_2$ 8.48550	78	<u>1,6,12,17,21,21</u>	$Cr_1$ 13.73279
39	3,8,13,15	$Cr_3$ 8.63869	79	<u>1,6,12,18,21,21</u>	$Cr_1$ 13.84553
40	<u>3,9,14,14</u>	$Cr_3$ 8.78617	80	<u>1,6,12,17,22,22</u>	$Cr_1$ 13.96137

Fig. 1

Different parts of 2D hexagonal lattice produce the basis for ground state configurations of the majority of dipole clusters (see Table I). Shown are examples of such basic groups of crystal shells. Four most symmetrical groups of three shells each is presented.

Fig. 2

Ground state configurations of dipole clusters: a)  $D_{44}$ ; b)  $D_{47}$ ; c)  $D_{52}$ ; d)  $D_{59}$ . Squares denotes particles with 5 nearest neighbors.

Fig. 3

Two possible breakups of cluster  $D_{62}$  into shells: a) in such a way as to maximize the number of completed  $Cr_4$  shells.<sup>10</sup> b) so that the outer shell be well - defined and closed.

Fig. 4

The second and the first (in the insert of the Figure) "derivatives" of specific energy  $\epsilon(N)$  with respect to  $N$ .

Fig. 5

Cluster  $D_{37}$ . a) The ground state configuration  $D_{37}(1, 6, \bar{1}, 13, 16)$ . b) the eigenvector of the cluster motion in the global minimum with the minimal nonzero eigenfrequency  $\omega_{min} \approx 0.58$  c) the picture of the motion in the lowest local minimum  $D_{37}^{(1)}(1, 7, 13, 16)$  with a minimal eigenfrequency  $\omega_{min}^{(1)} \approx 0.4$ . Five - coordinated particles are marked by squares.

Fig. 6

Minimal nonzero eigenfrequencies  $\omega_{min}$  for the normal modes of  $N$  - particle dipole clusters.

Fig. 7

Characteristic examples of normal motions with eigenfrequencies  $\omega_{min}$  (see Fig. 6). a)  $D_{10}$ ; b)  $D_{35}$ ; c)  $D_{55}$ ; d)  $D_{56}$ .

Fig. 8

The measure of faceting  $\nu_s(N)$  is shown for different shells  $s$ . Appropriate values for crystal shells of different types are plotted by thick solid lines.

Fig. 9

Three - shell cluster  $D_{24}(3, 8, 13)$ . The results of calculations of the mutual orientational parameter (10) and of deviations (5),(6) as functions of temperature  $T$  are presented. The data are connected to guide the eyes. If not present,

error bars are smaller than the size of the data point.

Fig. 10

Four - shell cluster  $D_{35}(1, 6, 12, 16)$ . Mutual orientational parameter  $Re|g_{32}|$  and relative deviations  $\delta_{pair}(T)$  vs. temperature  $T$ .

Fig. 11

Temperature dependence of excess energy  $\epsilon(T)$  for a number of dipole clusters  $D_N$ . In the insert the excess energy of  $D_{37}$  cluster in the temperature region  $T \in [0.02, 0.02]$  is shown.

Fig. 12

The magnitude of the first Bragg peak as a function of  $T$  for clusters  $D_{40}$  and  $D_{45}$ . Shown also is 2D topography of the structure factor  $S(\mathbf{k})$ ,  $S(\mathbf{k}) < 0.5$  at different temperatures. "Solidlike" to "liquidlike" transition is accomplished by the washing out of  $S(\mathbf{k})$  in regions  $\mathbf{k} \approx \mathbf{q}_1$  of reciprocal lattice vectors.

Fig. 13

The radial diffusion constant (7) vs. temperature  $T$ . The insert shows a typical diffusive motion of particles when the cluster is in disordered state ( $T \geq T_f$ ). Results of the linear fit (see Equation (7)) are also given.

Fig. 14

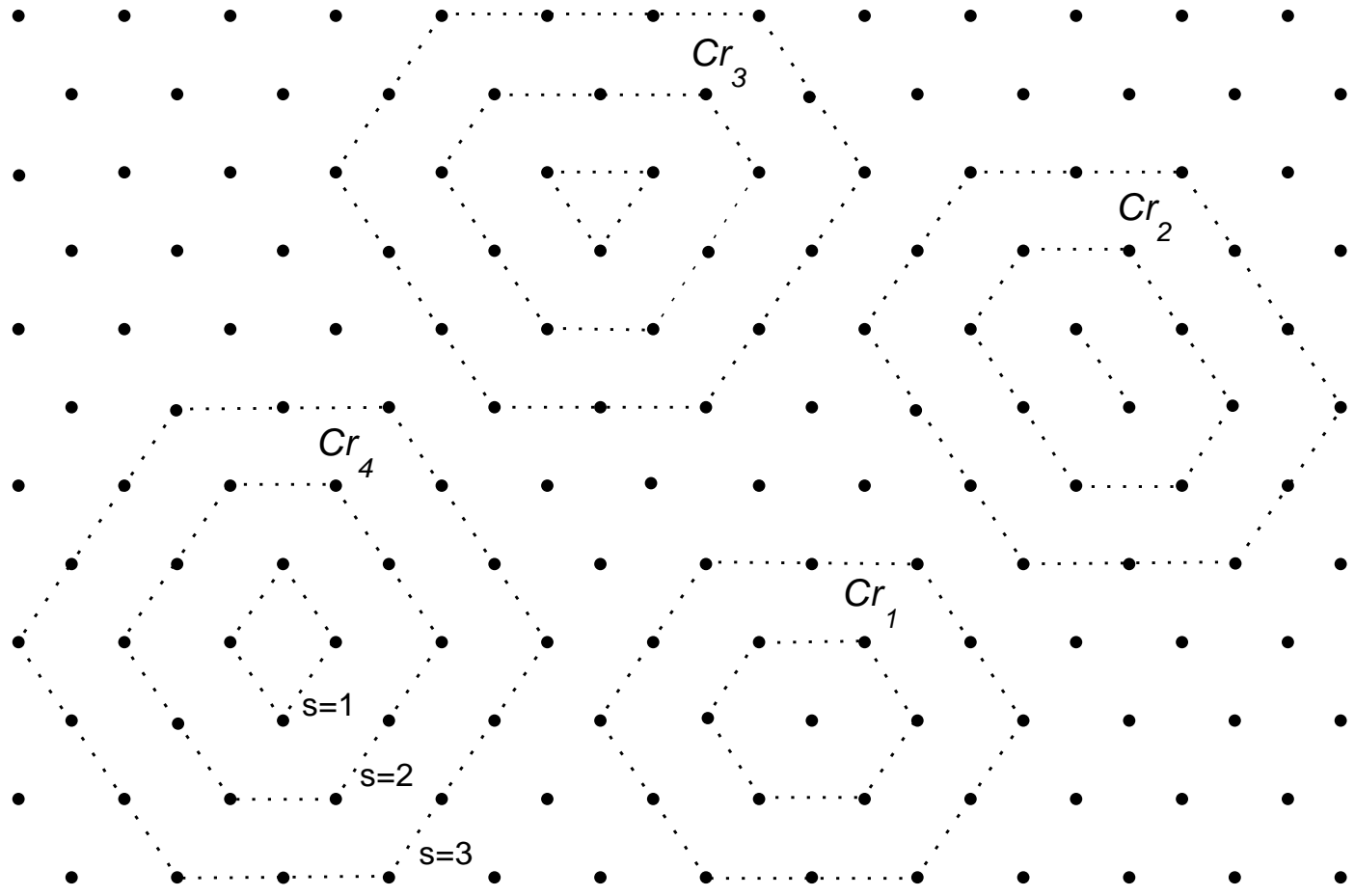
The total melting temperatures  $T_f(N)$  and scaled from "cluster" to "infinite system" temperatures  $T_f^{inf}(N)$  (11) as functions of number of particles  $N$ . Points correspond to the results of present simulations. The dotted line depicts a possible behavior of  $T_f^{inf}(N)$  at  $N > 50$ . Temperature of first - order phase transition in an infinite 2D dipole system  $T_c^{inf}$  is shown with the help of a dashed line. Temperature  $T_f^{inf}(N; r < r_c)$  of the disordering of a core is assumed to tend to  $T_c^{inf}$  as  $N$  increases.

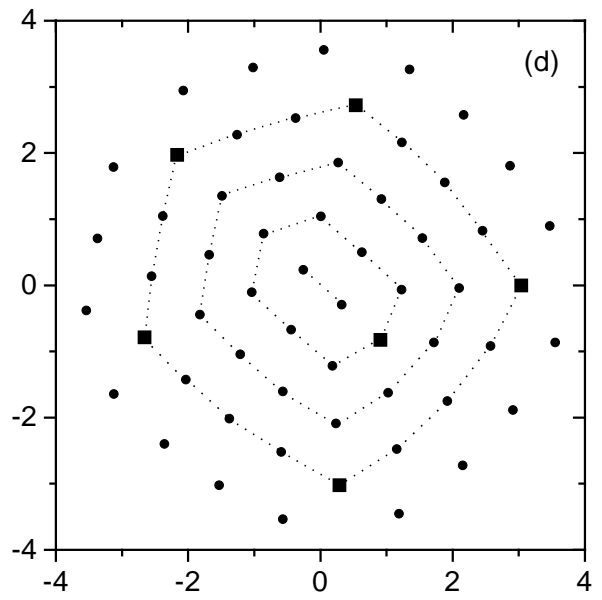
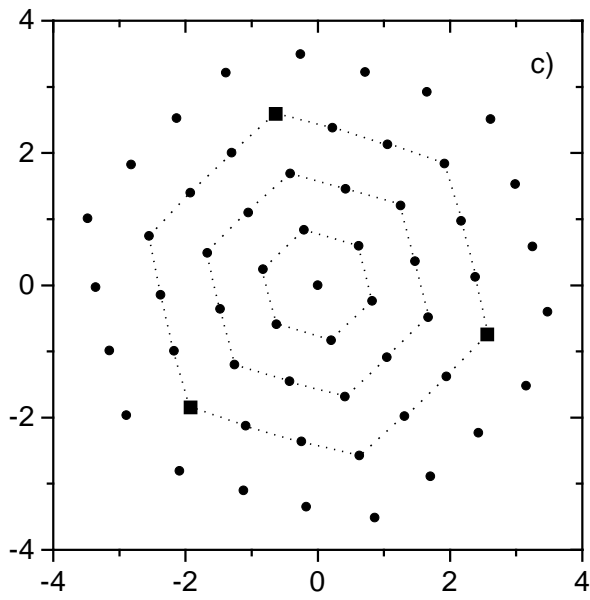
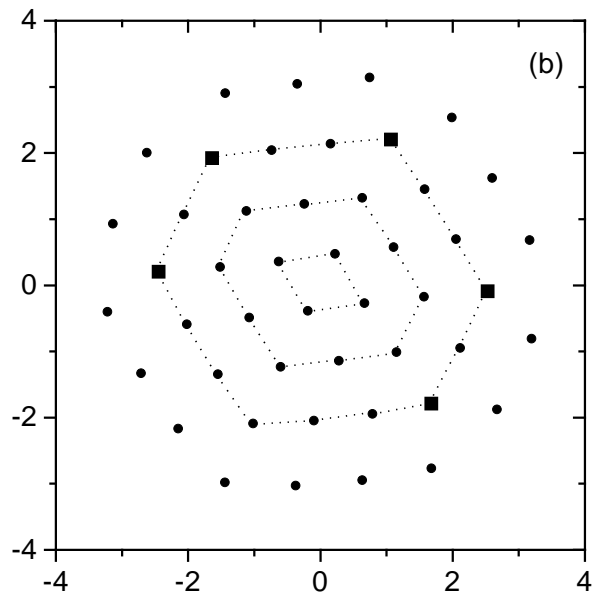
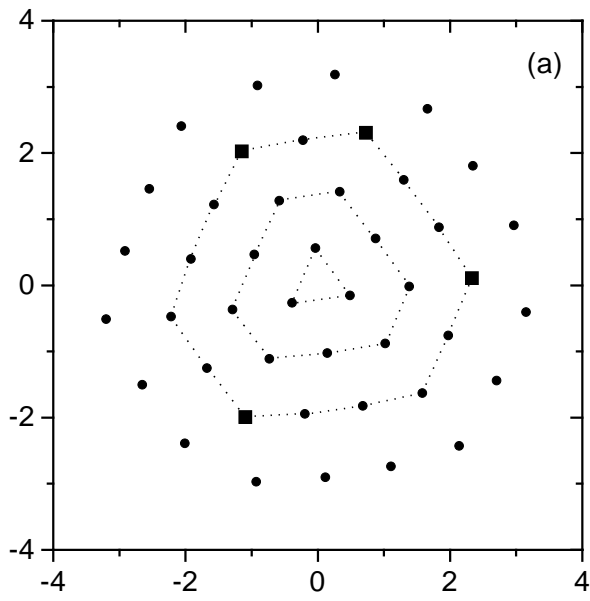
Fig. 15

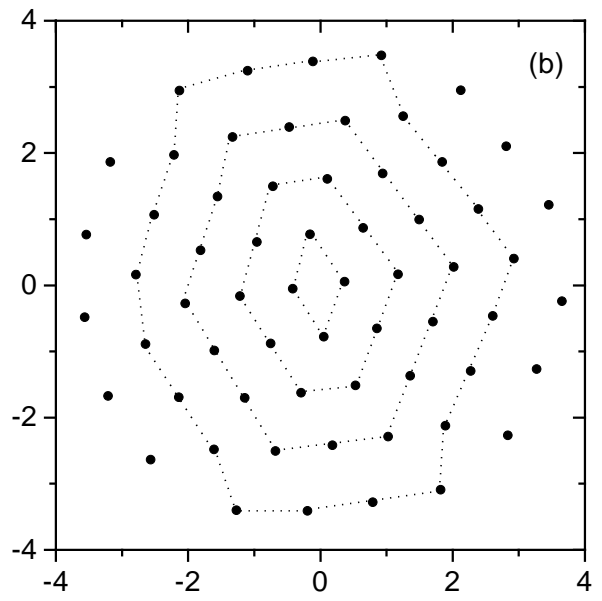
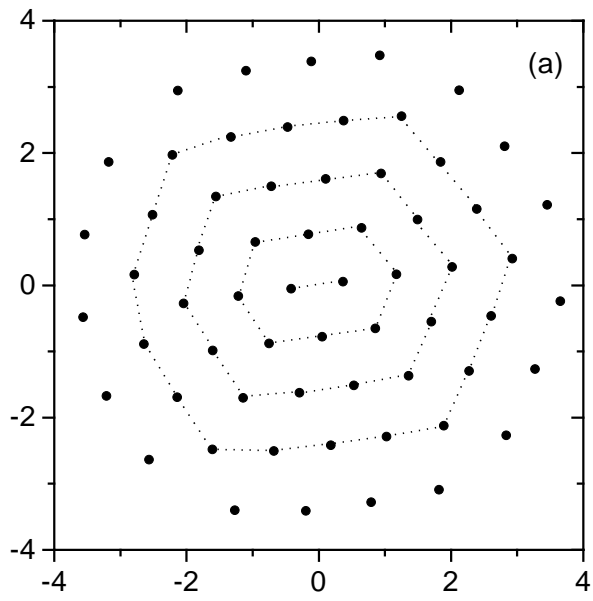
The probability that the central particle of cluster  $D_{37}$  has six neighbors as a function of temperature  $T$ . In the insert local minima distributions for different temperatures are shown. One can see that at  $T > 0.01$  a group of local minima with energies near  $\epsilon^{(1)}$ , the energy of the lowest local minimum, are being occupied.

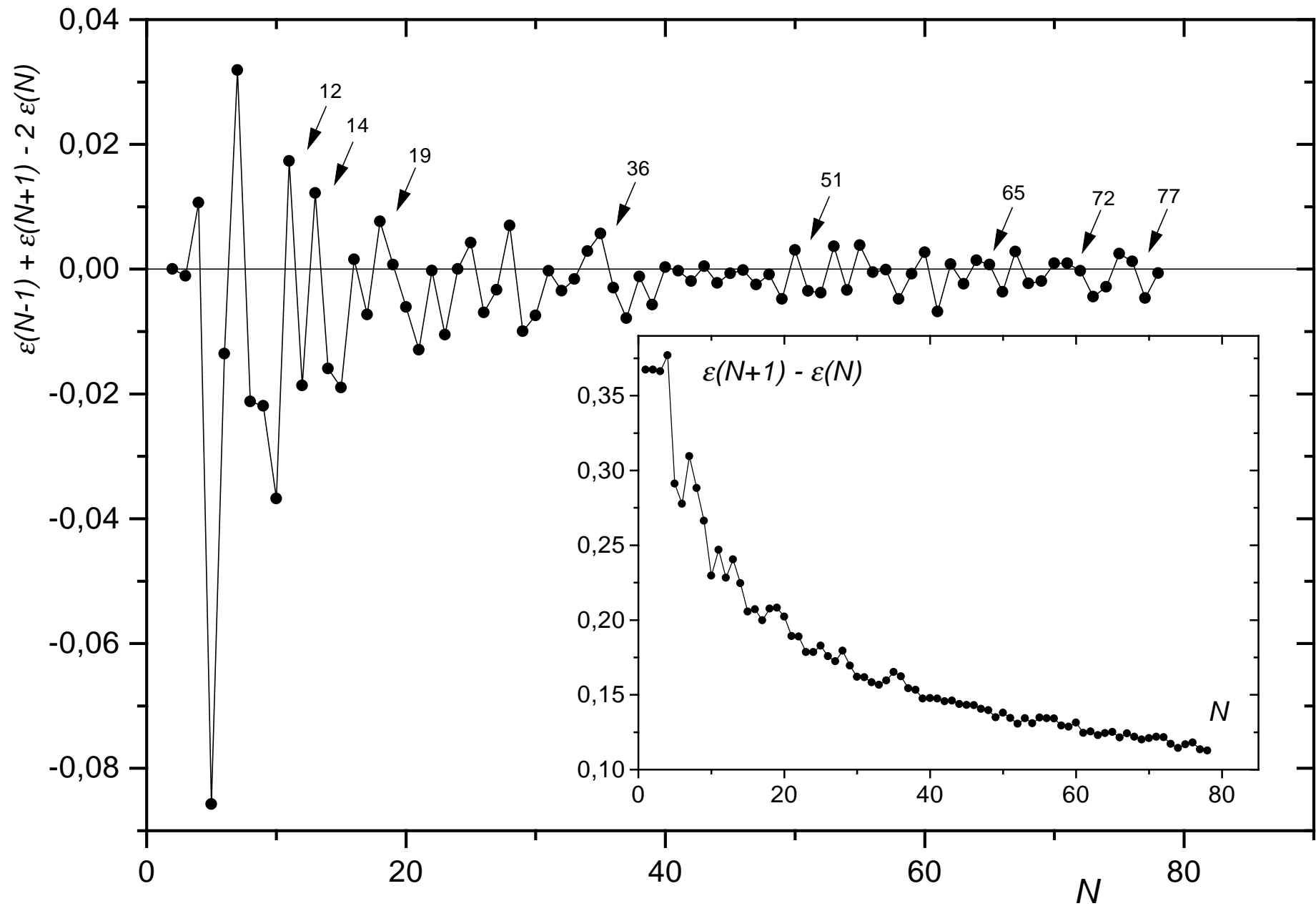
Fig. 16

Radial distribution function  $g(r)$  of cluster  $D_{37}$ .

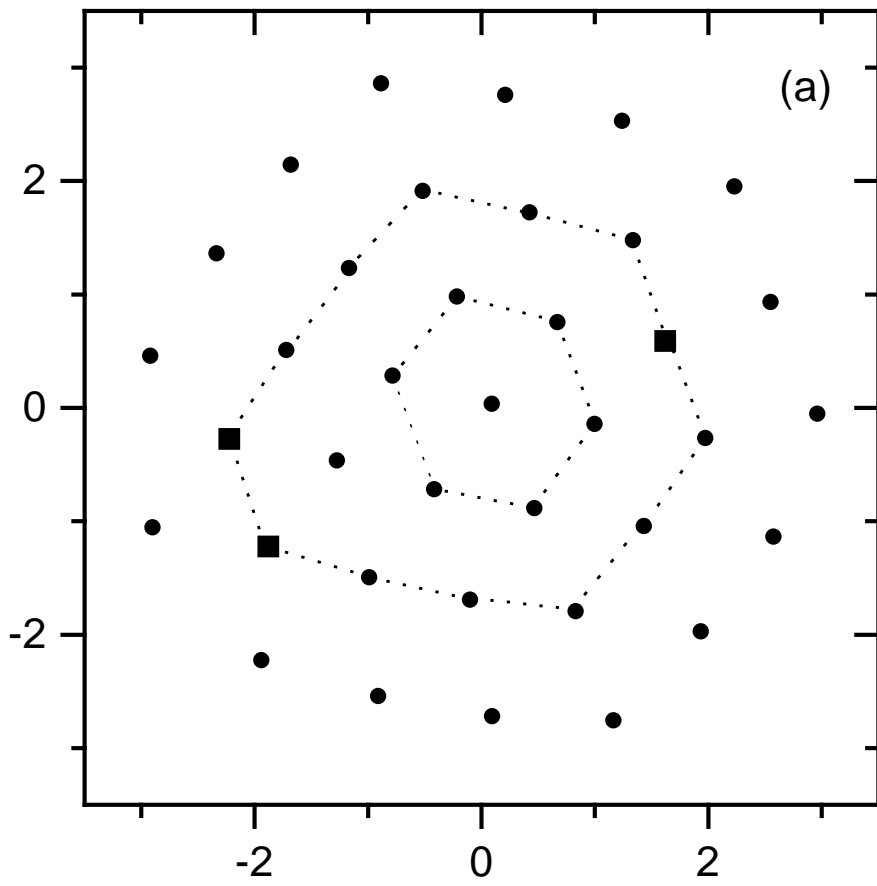




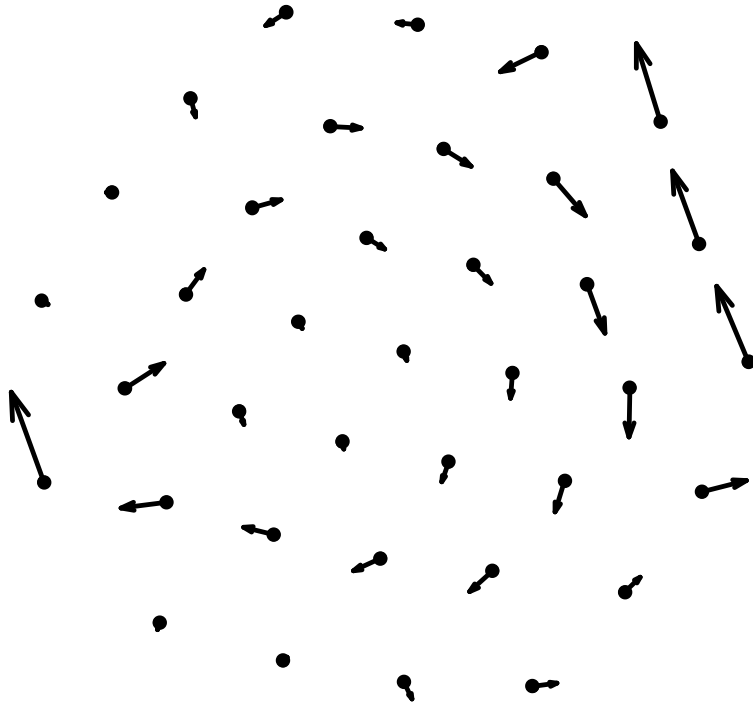




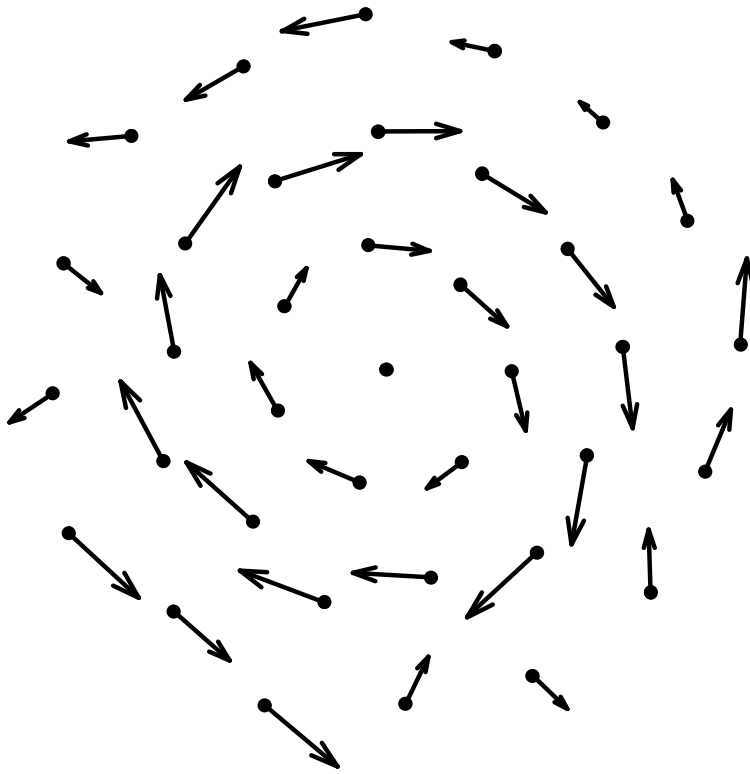


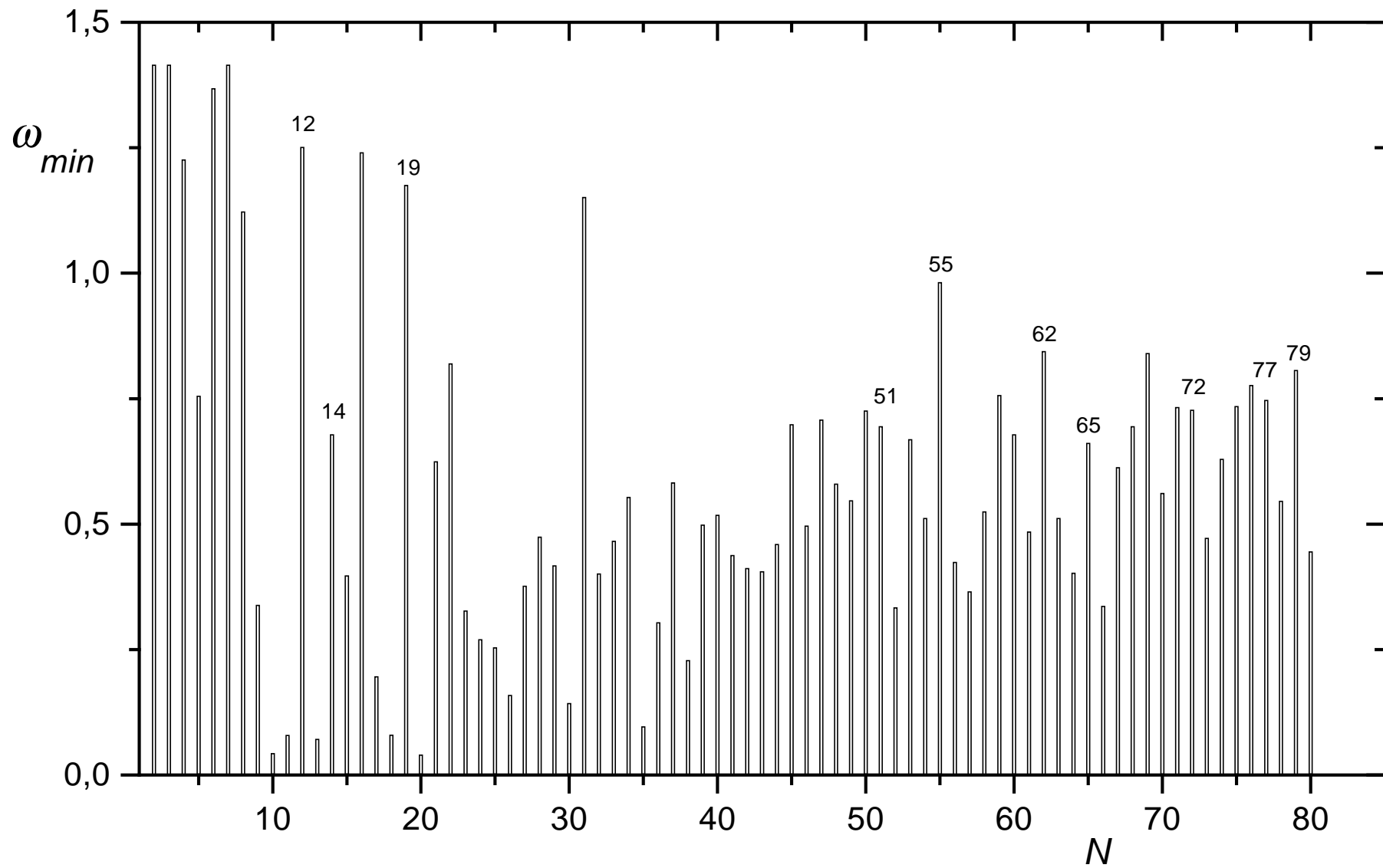


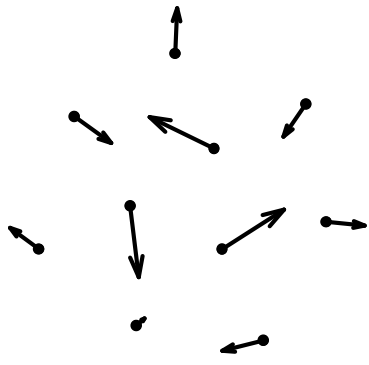
(b)



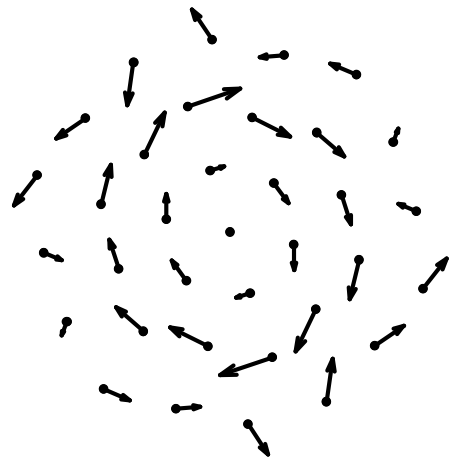
(c)



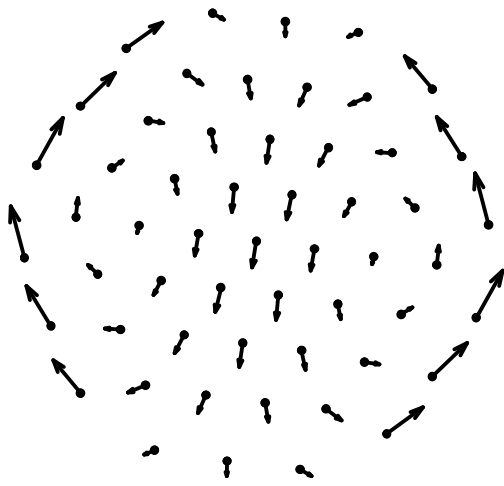




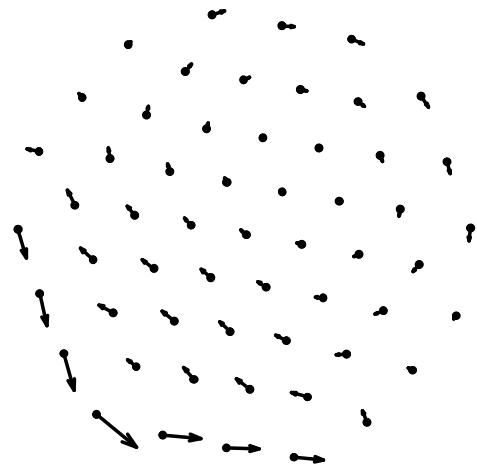
(a)



(b)



(c)



(d)

